USB Proceedings

IECON 2012 - 38th Annual Conference on IEEE Industrial Electronics Society

École de Technologie Supérieure de Montréal, Université du Québec
Montreal, Canada
25 - 28 October, 2012

Sponsored by

The Institute of Electrical and Electronics Engineers (IEEE)
IEEE Industrial Electronics Society (IES)

IECON 2012 - 38th Annual Conference on IEEE Industrial Electronics Society

IEEE Catalog Number: CFP12IEC-USB
ISBN: 978-1-4673-2420-5

Additional copies of this publication are available from

Curran Associates, Inc.
57 Morehouse Lane
Red Hook, NY 12571 USA
+1 845 758 0400
+1 845 758 2633 (FAX)
email: curran@proceedings.com

Comparison of current control for low harmonic distortion applied to a small wind generation system with permanent magnet synchronous generator

O. Carranza[1], E. Figueres[2], G. Garcerá[2], R. Ortega[1,2]
[1]Escuela Superior de Cómputo - Instituto Politécnico Nacional, Av. Juan de Dios Bátiz S/N, D. F., 07738, México.
[2]Departamento de Ingeniería Electrónica – UPV, Camino de Vera S/N, 7F, Valencia, 46022, España.
ocarranzac@ipn.mx, efiguere@eln.upv.es, ggarcera@eln.upv.es, rortegag@ipn.mx,

Abstract- This paper presents a comparison between of two type of current control to reduce the THD$_i$ and increase the PF in a Three-Phase Boost Rectifier driving a small wind turbine. **The two types of current controls are peak current mode control and average current mode control** ***It is used as the input stage of small wind turbines with permanent magnet synchronous generators operating at variable speed. The Boost Rectifier output is connected to an inverter which injects the energy to a distribution power grid. The operation in discontinuous conduction mode allows significantly reducing the Total Harmonic Distortion of the current in the small wind turbine. However, it is necessary to add an input filter so that the switching ripple doesn´t affect the turbine. The results demonstrate that it is better the peak current mode control, because it is achieved a smaller THD$_i$ and a higher PF in all over the operating range of the generator.***

I. INTRODUCTION

A Wind Generation System (WGS) is constituted by an eolic turbine and an electrical generator. In small WGSs it is preferred the use of Permanent Magnet Synchronous Generators (PMSG) operating at variable speed, so that both amplitude and frequency of the generator output voltage varies in a certain range, following the wind speed. Therefore a power converter is needed to connect the WGS to the distribution power grid.

The simplest converter to process the WGS energy is the cascade association of a non controlled rectifier, a DC-DC converter and a power inverter, which is connected to the grid [1]-[3].

With such a configuration, the harmonic distortion of the generator currents (THDi) is high, achieving THDi 30% [4]-[6]. In some works, a Boost DC-DC converter is used to regulate to a constant value the voltage at the input of the power inverter, in spite of the rectifier voltage reduction when the PMSG operates at low speeds. However, in this work, the input voltage of the inverter is controlled by the inverter, whereas the DC-DC converter regulates the current at the output of the rectifier. As a whole, the non controlled rectifier and the Boost DC-DC converter are known as Boost Rectifier, which can be also used to reduce the generator currents distortion [7]-[10]. Usually, a Boost Rectifier driving a PMSG operates in Continuous Conduction Mode (CCM), because of the large value of the generator inductances. Fig. 1 shows the current and voltage at the output of one of the generator phases of a Boost Rectifier working in CCM.

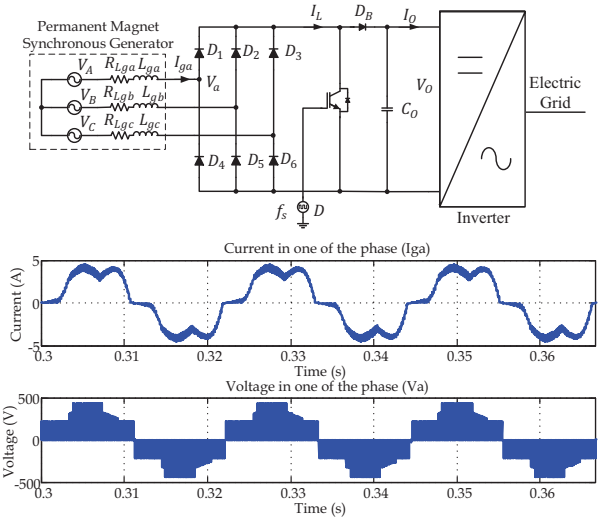

Fig. 1. Current and voltage of one phase of a three-phase boost rectifier in CCM.

Moreover, the current harmonics produce torque harmonics in the PMSG, resulting in additional vibrations and increasing the maintenance needs.

An outstanding novelty of this work with regard to [7]-[10] is that both the voltage amplitude and frequency vary in a wide operation range, which depends on the turbine speed.

As a result, both the power stage and the control loops of the Boost Rectifier must be carefully designed.

Current Injected-Mode Control (CIC) or Peak Current-Mode Control (PCC) [11] is the most widely used current mode control in switching power supplies, as it gives a strict adherence to the current in the inductor, which is highly recommended when working in DCM. PCC addition by controlling the peak current is controlled in the inductor or power active switch (power transistor), so that there is an inherent protection against overcurrent control.

Average Current-Mode Control (ACC) [12], is another widely used current mode control in power converters. In the ACC like PCC is sensed in the inductor current power to implement the current control loop, however, can also ACC reflecting another current sensing the inductor current. Changing the point of looking for sensing the signal contains less noise, primarily from the switching frequency. The other

point where it can sense the current is the output of the generator, at this point that leaves the current generator, depends on the current flowing in the coil power and has the advantage that contains less harmonic components of the frequency switching. In this case, the currents are measured generator.

II. BOOST RECTIFIER IN DCM

Fig. 2 shows the scheme of the Three-Phase Boost Rectifier in DCM. Table I shows the values of the prototype characteristics.

The circuit that is used for the analysis considers two phases during the time interval when 2 diodes of the non-controlled rectifier are conducting, considering $L_g = 2L_{ga}$, $R_{Lg} = 2R_{Lga}$, $L = 2L_a$, $R_L = 2R_{La}$ and $C_i = 3C_1/2$. V_i is the rectifier output voltage, without considering resistive losses, averaged in a complete period of rectification, as it is shown by Fig. 3. V_o is regulated by the grid connection inverter.

A. DC model of the boost rectifier in DCM

In order to work in discontinuous conduction mode (DCM) [13], condition (1) must be accomplished. This condition allows the design of L to operate in DCM in the whole range of PMSG speeds. D is the duty cycle, L is the equivalent Boost inductance, f_s is the switching frequency and T_s is $1/f_s$.

Table I. Characteristics of the prototype

Characteristics	Values
Nominal Output Power of the generator (P)	2 kW
Output Voltage of the Boost Rectifier (V_0)	650 V
Output voltage range of the generator (V_{ab})	104 - 416 V_{rms}
Inductance of one phase of the generator (L_{ga}, L_{gb}, L_{gc})	25 mH
Resistance of one phase of the generator (R_{ga}, R_{gb}, R_{gc})	5 Ω
Number of poles (n_p)	12
Nominal Current (I_{nom})	4.87 A_{rms}
Speed range of the generator (n_m)	150 – 600 rpm

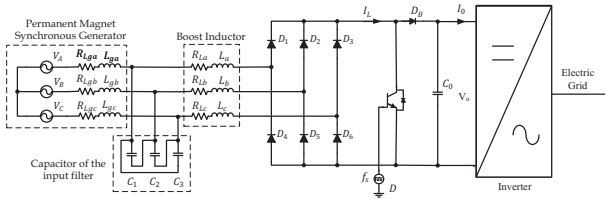

Fig. 2. Three-Phase Boost Rectifier in DCM.

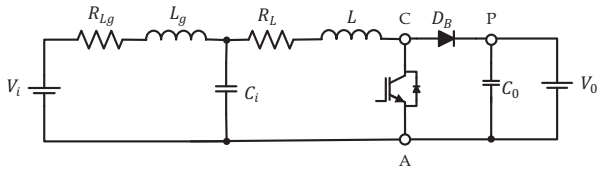

Fig. 3. Equivalent circuit of the boost rectifier.

$$\frac{2LP_0}{V_0^2 T_s} > (1-D)^2 D \quad \text{CCM}$$
$$\frac{2LP_0}{V_0^2 T_s} < (1-D)^2 D \quad \text{DCM} \tag{1}$$

The duty cycle in DCM is obtained from (2)

$$D = \sqrt{\frac{2LP_o(V_o - V_i)}{T_s V_o V_i^2}} \tag{2}$$

The maximum value of the Boost inductance (L_{max}) is obtained from (1) and (2). For a switching frequency (f_s) of 5 kHz, considering the generator speed range, it results L_{max} = 907.1 µH. L = 750 µH is selected, so that the Boost rectifier operates in DCM in the whole load range.

B. Input filter

An input LCL filter is used to filter out the components at the switching frequency in the generator currents, and also to achieve DCM. Note that because of the large value of the generator inductances, the operation in DCM of the Boost Rectifier is not possible if an additional LCL Filter is not used. The transfer function from the rectifier current to the generator current is determined by (3).

$$\frac{i_g(s)}{i_L(s)} = \frac{1}{s^2 C_i L_g + s C_i R_{Lg} + 1} \tag{3}$$

With C_i = 3.3µF, an attenuation of – 44.3 dB at the switching frequency (f_s = 5 kHz) is achieved by the filter.

C. Small-signal model of the boost rectifier in DCM

A small signal circuit of the Boost rectifier working in DCM can be obtained by means of the equivalent circuit of the PWM switch [14], as it is shown by Fig. 4. The output voltage (V_o) is regulated by the inverter connected to the grid, so that the load that is 'seen' by the Boost Rectifier can be modeled as a constant voltage source. Therefore in the small-signal circuit $\hat{v}_0$ is the disturbance in the output voltage.

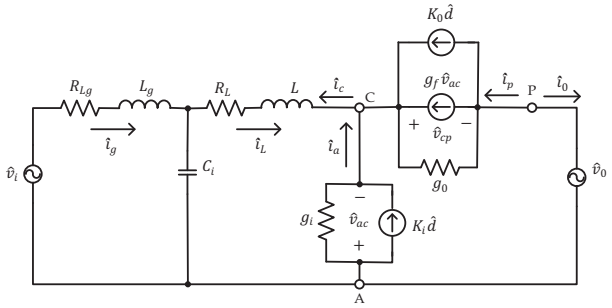

Fig. 4. Small Signal Equivalent Circuit of the Boost Rectifier with voltage source in the output

The values of the parameters of the PWM switch in DCM are shown by (4).

$$g_i = \frac{D^2 T_s}{2L} \qquad g_o = \frac{2LP_o^2}{D^2 V_g^2 V_o^2 T_s} \qquad g_f = \frac{2P_o}{V_g V_o}$$
$$K_i = -\frac{DT_s V_g}{L} \qquad K_o = -\frac{2P_o}{DV_o} \tag{4}$$

In order to design the control loop, the duty cycle to Boost inductor current transfer function, $G_{id}(s) = \hat{\imath}_L(s)/\hat{d}(s)$, is needed if the current loop is closed by sensing the Boost inductor current. This transfer function is shown by (5). It is shown by Fig. 5

$$G_{id}(s) = \frac{\hat{\imath}_L(s)}{\hat{d}(s)} = \frac{-\left(s^2 C_i L_g + sC_i R_g + 1\right)(K_i + K_o)}{s^3 B_3 + s^2 B_2 + sB_1 + B_0}$$
$$B_3 = C_i L_g L\left(g_i + g_o + g_f\right)$$
$$B_2 = C_i\left[L_g + \left(g_i + g_o + g_f\right)\left(LR_{L_g} + L_g R_L\right)\right] \tag{5}$$
$$B_1 = \left[C_i R_{L_g} + \left(g_i + g_o + g_f\right)\left(L_g + L + C_i R_L R_{L_g}\right)\right]$$
$$B_0 = \left(g_i + g_o + g_f\right)\left(R_{L_g} + R_L\right) + 1$$

As an alternative, the duty cycle to the generator currents transfer function, $G_{gd}(s) = \hat{\imath}_g(s)/\hat{d}(s)$, must be used if the current loop is closed by sensing the generator currents. This transfer function is shown by (6). It is shown by Fig. 6.

$$G_{gd}(s) = \frac{\hat{\imath}_g(s)}{\hat{d}(s)} = \frac{(K_i + K_o)}{s^3 B_3 + s^2 B_2 + sB_1 + B_0}$$
$$B_3 = C_i L_g L\left(g_i + g_o + g_f\right)$$
$$B_2 = C_i\left[L_g + \left(g_i + g_o + g_f\right)\left(LR_{L_g} + L_g R_L\right)\right] \tag{6}$$
$$B_1 = \left[C_i R_{L_g} + \left(g_i + g_o + g_f\right)\left(L_g + L + C_i R_L R_{L_g}\right)\right]$$
$$B_0 = \left(g_i + g_o + g_f\right)\left(R_{L_g} + R_L\right) + 1$$

The Bode plots of these transfer functions are shown by Fig. 5 and Fig. 6, with L = 750 µH and the values of the elements that have been previously described. From this figure it may be deduced in the case ACC, the convenience of measuring the generator currents instead of the DC current, because the resonance of the LCL filter complicates the control loop stabilization with practical crossover frequency values of the current loop.

III. PEAK CURRENT-MODE CONTROL

Fig. 7 shows the block diagram of the current loop with PCC [10]. The reference for the current loop, $I_{control}$, is provided by the controller of the speed control loop.

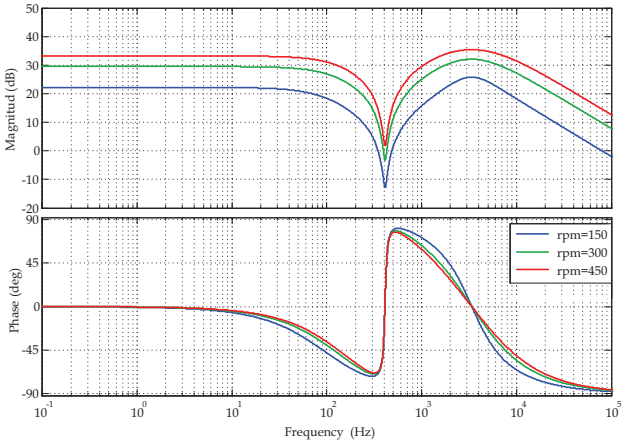

Fig. 5. Transfer Functions of $\boldsymbol{G_{id}(s)}$.

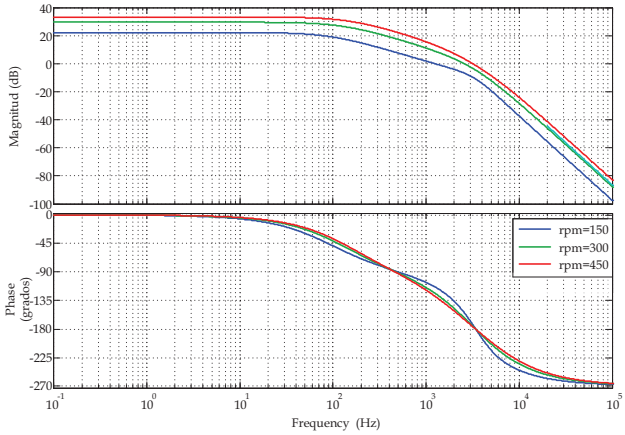

Fig. 6. Transfer Functions of $\boldsymbol{G_{gd}(s)}$.

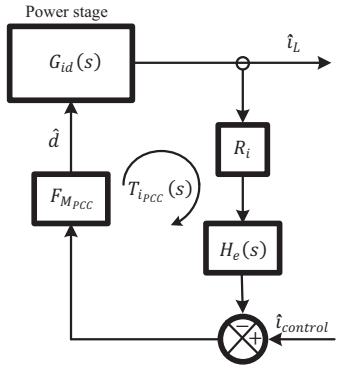

Fig. 7. Scheme of Peak Current-Mode Control.

The loop gain of the current loop, $T_{i_{PCC}}(s)$, is expressed by **(7)**. R_i=0.015 is the current sense gain, $F_{M_{PCC}}$ is the PWM modulator gain, and $H_e(s)$ is the sampling gain [11], typical in peak current mode control.

$$T_{i_{PCC}}(s) = G_{id}(s) H_e(s) R_i F_{M_{PCC}} \tag{7}$$

The sampling gain $H_e(s)$ is expressed by (8)

$$H_e(s) = 1 + \frac{s}{\omega_z Q_z} + \frac{s^2}{\omega_z^2} \tag{8}$$

Where

$$\omega_z = \frac{\pi}{T_s} \qquad \text{and} \qquad Q_z = -\frac{2}{\pi}$$

In order to guarantee the stability of the current loop, the PWM modulator gain, $F_{M_{PCC}}$, expressed by (9), should be adjusted properly.

$$F_{M_{PCC}} = \frac{1}{(S_n + S_e)T_s} \tag{9}$$

In (9) S_n is the on-time slope of the current sense waveform, S_n is the slope of the stabilization ramp, S_e = 22.503 V/ms. The value of S_n is obtained from (10).

$$s_n \approx \frac{V_i}{L} R_i \tag{10}$$

The PCC implementation is shown by Fig. 8. For the implementation using the UC3823 Integrated Circuit, which has implemented the PWM modulator circuit PCC. In this circuit is only shown the PCC control, however, the circuit contains all other elements for its proper functioning.

IV. Average Current-Mode Control

The control loop structure of ACC [12] for this converter is shown by Fig. 9.

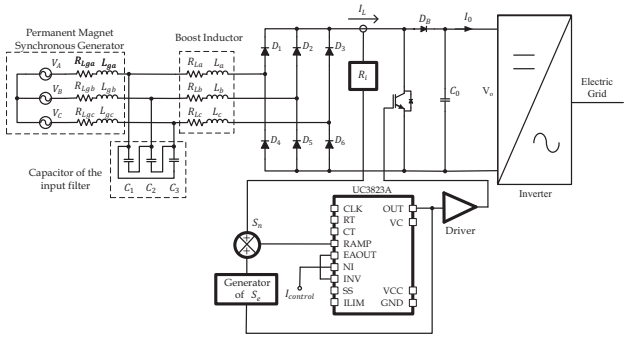

Fig. 8. DCM Three Phase Boost Rectifier with PCC Control.

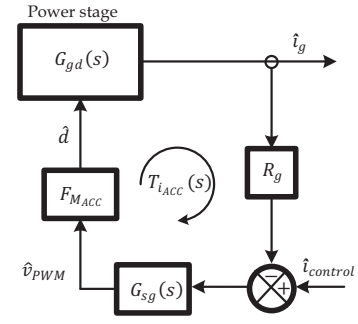

Fig. 9. Scheme of Average Current Mode Control.

The loop gain of the current loop, $T_{i_{ACC}}(s)$, is expressed by (11).

$$T_{i_{ACC}}(s) = G_{gd}(s) G_{sg}(s) R_g F_{M_{ACC}} \tag{11}$$

R_g=0.2 is the current sense gain and $F_{M_{ACC}}$ is the PWM modulator gain, expressed by (12)

$$F_{M_{ACC}} = \frac{1}{S_e T_s} \tag{12}$$

S_e is external slope, S_e = 5 V/ms. The compensator $G_{sg}(s)$ is designed to stabilize the current control loop, $T_{i_{ACC}}(s)$, with a phase margin higher than 50° and a gain margin higher than 7 dB. The compensator $G_{sg}(s)$ is expressed by (13)

$$G_s(s) = \frac{\omega_{is}\left(1 + \frac{s}{\omega_{zs}}\right)}{s\left(1 + \frac{s}{\omega_{ps}}\right)} \tag{13}$$

The compensator $G_{sg}(s)$ that guarantees the stability of the current loop is expressed by (14)

$$G_{sg}(s) = \frac{300(s + 754)}{s(s + 3141)} \tag{14}$$

The ACC implementation is shown by Fig. 10. To close the ACC loop by measuring the generator currents, a signal processing is required to calculate the average value of the equivalent rectified currents of the generator. Note that only two currents are sensed, because the PMSG currents make up a 3 wire system. The signal processing has been implemented by means of a C Script Block of PSIM [17], in a similar way that it will be implemented in the experimental prototype.

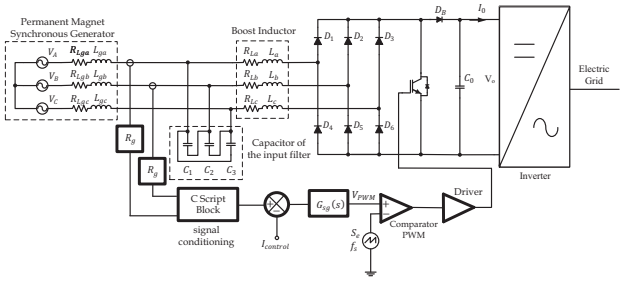

Fig. 10. DCM Three Phase Boost Rectifier with ACC Control measuring the DC current at the output of the rectifier.

V. Simulated Results

The performance of the proposed control loops has been evaluated by means of the PSIM 7.0.5 software [16].

Fig. 11 shows both current and voltage at the output of one of the generator phases when using the PCC control. Fig. 12 shows both current and voltage at the output of one of the generator phases when using the ACC control. In both

figures, the generator speed is 450 rpm and the rectifier output power is 2 kW. In these figures, it is observed that there is less THDi when used PCC control.

Fig. 13shows the measured generator THDi and PF of the PMSG in the whole speed operation range. The maximum power of the generator, which is limited by the nominal current at low speeds, is also shown.

Fig. 13 that the improvement of the THDi and PF values is better when it is used PCC control, although for some the speed is similar THDi.

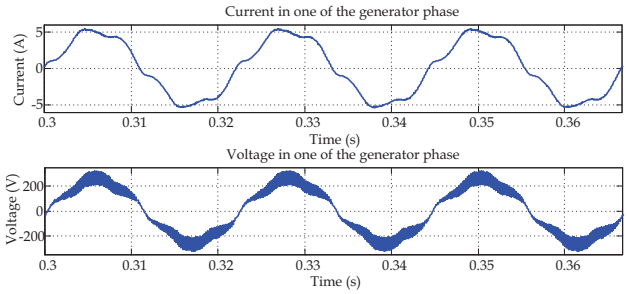

Fig. 11. Current and Voltage of one phase of the DCM Three-Phase Boost Rectifier with PCC Control in simulation.

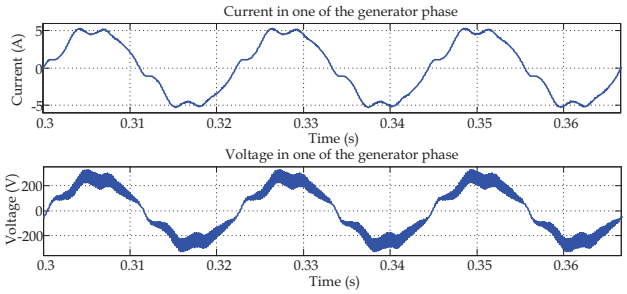

Fig. 12. Current and Voltage of one phase of the DCM Three-Phase Boost Rectifier with ACC Control in simulation.

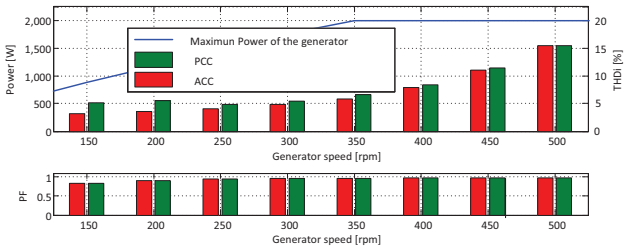

Fig. 13. Comparison of the measured THDi and PF in PCC vs. ACC in simulation.

VI. Experimental Results

The three-phase DCM boost rectifier WECS has been implemented in an experimental prototype. The 2 kW PMSG is connected to a commercial AC motor drive Siemens Micromaster 440 that feeds a 5.5 kW induction motor 1LE1002CC322AA4Z from Siemens. This AC motor is connected to the PMSG.

The PCC of the boost converter has been implemented with the integrated circuit UC3823. The ACC control has been implemented by means of a DSP TMS320F28335.

Fig. 14 shows both current and voltage at the output of one of the generator phases when using the PCC control. Fig. 15 shows both current and voltage at the output of one of the generator phases when using the ACC control. In both figures, the generator speed is 450 rpm and the rectifier output power is 2 kW. In these figures, it is observed that there is less THDi when used PCC control.

Fig. 16shows the measured generator THDi and PF of the PMSG in the whole speed operation range. The maximum power of the generator, which is limited by the nominal current at low speeds, is also shown.

Fig. 16 that the improvement of the THDi and PF values is better when it is used PCC control. In the experimental case, it is observed in greater detail the difference PCC control when used in comparison with the control ACC.

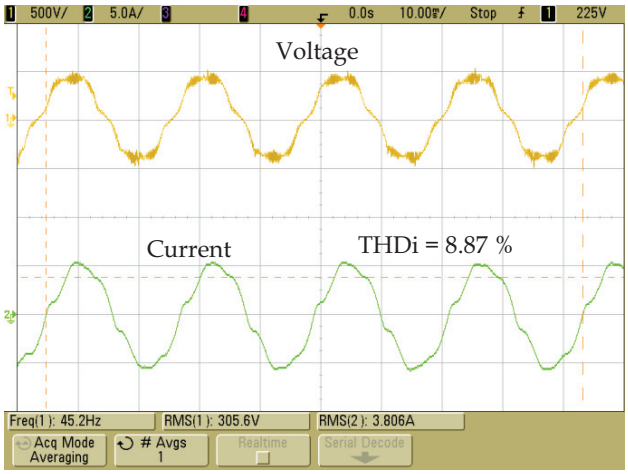

Fig. 14. Current and Voltage of one phase of the DCM Three-Phase Boost Rectifier with PCC Control in experimental.

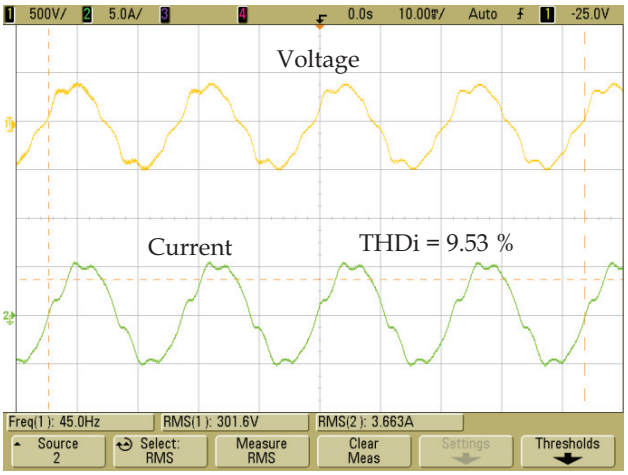

Fig. 15. Current and Voltage of one phase of the DCM Three-Phase Boost Rectifier with ACC Control in experimental.

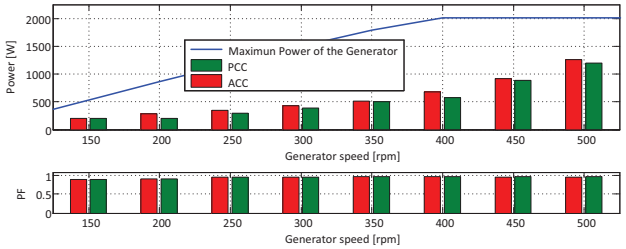

Fig. 16. Comparison of the measured THDi and PF in PCC vs. ACC in experimental.

VII. Conclusion

In this paper it has been presented a comparison between of two type of current control to reduce the THDi and increase the PF in a Three-Phase Boost Rectifier driving a small wind turbine. In PCC control implementation, analysis was performed in order to ensure the stability of current control loop by selecting the appropriate value of the external ramp. In the ACC control implementation, analysis was performed in order to stabilize the control loop current through the appropriate compensator.

To determine which of the two controls yields a lower THDi and higher PF, the simulation is performed Boost Rectifier | with each of the controls through the PSIM. To confirm the simulated results were performed an experimental evaluation of the Boost rectifier using control PCC and ACC control. The range of speeds at which they were tested was 150 to 500 rpm.

The results demonstrate that it is better the peak current mode control, because it is achieved a smaller THDi and a higher PF in all over the operating range of the generator.

In the experimental case, Boost rectifier with PCC control achieves low THDi (1.93 % - 11.97 %) and high PF (0.9 – 0.98) in comparison with the Boost Rectifier with ACC control (THDi = 2.15 % - 12.7 % and PF = 0.9 – 0.98).

Acknowledgment

The first author thanks the support of the Instituto Politécnico Nacional (IPN) and of the Comisión de Operación y Fomento de Actividades Académicas (COFAA) to finance his stay in the Universidad Politécnica de Valencia (UPV).

References

[1] Naoki Yamamura, Muneaki Ishida, Takamasa Hori,"A simple Wind Power System With Permanent Magnet Type Synchonous Generator", *IEEE 1999 International Conference on Power Electronics and Drive Systems, PEDS'99*, pp. 849-854, July 1999.

[2] A.E. Haniotis, K.S. Soutis, A.G., Kladas, J.A. Tegopoulos, "Grid connected variable speed wind turbine modeling, dynamic performance and control", *Power Systems Conference and Exposition, 2004 IEEE PES*, pp. 759 – 764, vol.210-13 Oct. 2004

[3] Jamal A. Baroudi, Venkata Dinavahi, Andrew M. Knight, "A review of power converter topologies for wind generators" *Renawable Energy 32*, pp. 2369-2385, 2007.

[4] Ali M. Eltamaly, "Harmonics reduction of three-phase boost rectifier by modulating duty ratio", *Electric Power Systems Research 77*, pp. 1425–1431, 2007

[5] F.S. dos Reis, J.A.V. Ale, F.D. Adegas, R. Tonkoski, S. Slan, K. Tan, "Active Shunt Filter for Harmonic Mitigation in Wind Turbines Generators", *37th IEEE Power Electronics Specialists Conference*, PESC '06, 2007.

[6] J. Tsai, K. Tan, "H APF harmonic mitigation technique for PMSG wind energy conversion system", Universities Power Engineering Conference, 2007. AUPEC 2007. Australasian, 9-12 Dec. 2007.

[7] Y. Jang, M. M. Jovanovic, "A New Input-Voltage Feedforward Harmonic-Injection Technique Nonlinear Gain Control for Single-Switch, Three-Phase, DCM Boost Rectifiers" *IEEE Trans. on Power Electronics*, vol. 20, no. 1, pp. 268-277, March 2000.

[8] P. Barbosa, F. Canales, J. C. Crebier, F.C. Lee, "Interleaved Three-Phase Boost Rectifiers Operated in the Discontinuous Conduction Mode: Analysis, Design Considerations and Experimentation" *IEEE Trans. on Power Electronics,* vol. 16, no. 5, pp. 724-734, September 2001.

[9] S.M. Bashi, N. Mariun, S.B. Noor and H.S. Athab, "Three-phase Single Switch Power Factor Correction Circuit with Harmonic Reduction", *Journal of Applied Sciences 5 (1)*: pp. 80-84, 2005.

[10] *R. Ghosh, G. Narayanan,* "A Single-Phase Boost Rectifier System for Wide Range of Load Variations", *IEEE Transactions on Power Electronics*, VOL. 22, NO. 2, pp. 470-479, March 2007

[11] R. B. Ridley, "A new, continuous-time model for current-mode control [power convertors]", IEEE Trans. on Power Electronics, Vol. 6, No. 2, pp. 271-280, April 1991.

[12] J. M. Benavent,E. Figueres, G. Garcera, M. Pascual, "Robust model-following regulator for average current-mode control of boost DC-DC converters", *Proceedings of the IEEE International Symposium on Industrial Electronics*, ISIE 2005, 2005

[13] Robert W. Erickson, Dragan Maksimovic, *Fundamentals of Power Electronics*, USA, Kluwer Academic Publishers, 2001.

[14] V. Vorperian, "Simplified analysis of PWM converters using model of PWM switch I and II" *IEEE Trans. on Aerospace and Electronic Systems,* vol. 26, no. 3, pp. 490-505, may 1990.

[15] W. Tang, F. C. Lee, R. B. Ridley, "Small-Signal Modeling of Average Current-Mode Control", *IEEE Trans. on Power Electronics*, vol. 8, no. 2, pp. 112-119, April 1993.

[16] R. B. Ridley, "A new, continuous-time model for current-mode control [power convertors]", *IEEE Trans. on Power Electronics*, vol. 6, no. 2, pp. 271-280, April 1991.

[17] PSIM 7.0 User´s Guide (2006), Powersim Inc., March 2006.